Journal of Fluorescence, Vol. 8, No. 1, 1998

Probing the Relation Between Protein Structure and Intrinsic Tryptophan Fluorescence Using Superrepressor Mutants of the *trp* Repressor

Shyam Vangala,[1] Gediminas A. J. Vidugiris,[1] and Catherine A. Royer[1,2]

Received January 21, 1997; accepted August 15, 1997

The wavelength dependence of the intrinsic tryptophan fluorescence lifetime of a series of mutants of the *trp* repressor protein was characterized in both the native and the denatured states. These mutants belong to a particular class, called superrepressors, as their phenotype, when expressed *in vivo*, is to repress transcription at lower concentrations of the corepressor, tryptophan. It has been demonstrated previously that these mutations result in distinct and profound modifications of the structural and dynamic properties of the protein [Reedstrom and Royer (1995) *J. Mol. Biol.* **253**, 266; Reedstrom *et al.* (1996) *J. Mol. Biol.* **264**, 32; Smith *et al.* (1995) *Biochemistry* **34**, 13183]. The present observations reveal that in the native state, these structural and dynamic modifications result in subtle, yet significant alterations in the intrinsic tryptophan fluorescence decay characteristics. Surprisingly, significant differences in the fluorescence decays between the mutants and the wild-type protein were also observed for the guanidine hydrochloride unfolded states. These results are discussed in terms of the various models which have been proposed to explain the decay properties of tryptophan in proteins.

KEY WORDS: Fluorescence lifetimes; *trp* repressor; tryptophan; superrepressors.

INTRODUCTION

The fluorescence properties of the intrinsic tryptophan fluorescence of proteins represents a widespread and popular tool for the study of protein conformational changes due to important biological events such as macromolecular complexation, interactions with small ligands, and protein folding. Fluorescence has proven useful in such studies due to its extreme sensitivity to the environment, as well as its high signal-to-noise ratio in the range of biologically meaningful concentrations. Despite its widespread use in molecular biophysics, the structural and dynamic determinants of the intrinsic tryptophan fluorescence characteristics of proteins are not entirely understood.

A large number of studies have been published on the fluorescence properties of indole derivatives, tryptophan-containing peptides, and single tryptophan proteins that have brought to light some general rules (e.g., see Refs. 1–6). While *N*-acetyltryptophanamide (NATA) exhibits single exponential fluorescence decay characteristics (τ near 3 ns at room temperature) [7], the analysis of the decay of tryptophan-containing peptides and proteins often requires three or more components for acceptable fits. The origin of these multiple decay components has been proposed to arise from an equilibrium distribution (on the fluorescence time scale) of multiple rotamer populations of the indole moiety of the χ^1 and

[1] School of Pharmacy, University of Wisconsin—Madison, Madison, Wisconsin 53706.

[2] To whom correspondence should be addressed at Centre de Biochimie Structurale, INSERM U414, 15 ave. Charles Flahault, 34060 Montpellier Cedex 01, France. e-mail: royer@tome.cbs.univ-montp1.fr

1053-0509/98/0300-0001$15.00/0

χ^2 dihedral angles about the Cα–Cβ and Cβ–Cγ bonds leading to heterogeneous intensity decays due to interactions between the indole moiety and the peptide [1,2,8]. For example, in studies of the tryptophan-containing peptide, oxytocin, the amplitudes of the fluorescence decay times correlated well with the χ^1 rotamer populations determined by NMR [9]. Using small alanine-rich, helix-forming peptides, a correlation was observed for the amplitudes of the three fluorescence decay times of the single tryptophan residue and the α-helical content of the peptide as controlled by the concentration of denaturant [10]. Since the rotamer populations are related to the helical content, a relationship was inferred between rotamer populations and fluorescence decay characteristics. In addition to correlations with rotamer populations, Bismuto *et al.* [11] demonstrated that the heterogeneity of tryptophan decay in peptides was linearly correlated with the logarithm of the number of amino acids in the peptide.

The fluorescence decay characteristics of proteins can be more or less complex than those observed for peptides. Often, three (or even four) lifetime components are necessary to properly fit tryptophan decay in proteins, and the three most prominent decays often exhibit values near 5, 2, and 0.5 ns [12–14], the fourth, when resolved, being less than 200 ps. These lifetime values are the same as those recovered from the studies of tryptophan-containing peptides. The suggestion has been made, therefore, that the fluorescence properties of native proteins are dominated by the tryptophan rotamer populations, as well [10]. A more general approach has been to assume a distribution of conformational states implicating the entire structure, as opposed to rotamer populations of the tryptophan residue [15]. Bajzer and Prendergast [16] have suggested that the heterogeneous decay in proteins arises from the existence of multiple through-space quenching moieties with different quencher probabilities, such that no dynamics, either slow or fast, on the fluorescence time scale and no conformational heterogeneity need be invoked. Finally, Van Gilst and Hudson [17] have suggested that the forward and reverse reactions of exciplex formation between tryptophan and neighboring quenchers gives rise to heterogeneous decay.

We have been interested in the structural determinants of intrinsic tryptophan fluorescence of proteins for some time, since we, like others, use this observable extensively in the study of protein solution behavior. We have characterized the intrinsic tryptophan fluorescence of the *trp* repressor (TR), a dimeric protein containing two tryptophan residues per monomer. Using single tryptophan mutants, the individual contribution of each tryptophan to the total fluorescence decay in both the native and denatured states has been resolved [18–20]. In the present work, in an examination of the effects of structural perturbations observed for functional mutants on the fluorescence decay of proteins, we have characterized the fluorescence of a series of superrepressor mutants of TR that have been shown to exhibit altered secondary, tertiary, and quaternary structural properties with respect to the wild type [21–23].

Figure 1a shows a ribbon diagram of the three-dimensional structure of the apo (unliganded) form of TR [24], with the two intrinsic tryptophan residues, 19 and 99, labeled W99 and W19 A and B for each chain, respectively. This protein is nearly entirely α-helical, although it is now well established that the helical content in solution is lower than expected from the structure derived from crystallographic studies [24] and that the binding of tryptophan likely causes the DNA reading heads, helices D and E (at the top in Fig. 1a) to become more ordered [21–23,25,26]. The dimer interface is formed by the interlocking of helices A, B, and C from both monomers and the folding back of the C-terminal helix F bearing tryptophan 99 on this interlocked core.

One of the two tryptophan residues, 19, is found near the C-terminal end of helix A and the other, 99, in the middle of helix F, and both are located in interfacial regions between the two monomers, making contact with residues from the opposite subunit. The fluorescence decay of tryptophan 19, which is buried in the central core of the protein, exhibits a very blue-shifted emission with two decay components, one near 4–5 ns and the other near 2.5 ns [18]. No short component is observed for this tryptophan. Tryptophan 19 shows almost no depolarization due to local motions [20], and its average lifetime in the wild type is shorter than expected from that observed for its single tryptophan mutant due to the transfer of energy to tryptophan 99 [20]. Tryptophan 99, on the other hand, exhibits redder emission and two lifetime components at 2.5 and 0.5 ns. The shorter component disappears upon unfolding of the protein. We proposed that this component arises from quenching of tryptophan 99 by one of two asparagine residues from the opposite subunit [18,19].

Figure 1b shows the positions of four single-site superrepressor mutations studied here and first isolated by Yanofsky and co-workers for their ability to repress transcription *in vivo* at lower concentrations of the corepressor, tryptophan [27]. The first three are glutamate-to-lysine substitutions at positions 13, 18, and 49, while the last is an alanine-to-valine substitution at position 77 in the turn between the two helices, D and E, of the helix–turn–helix DNA binding motif. We and others

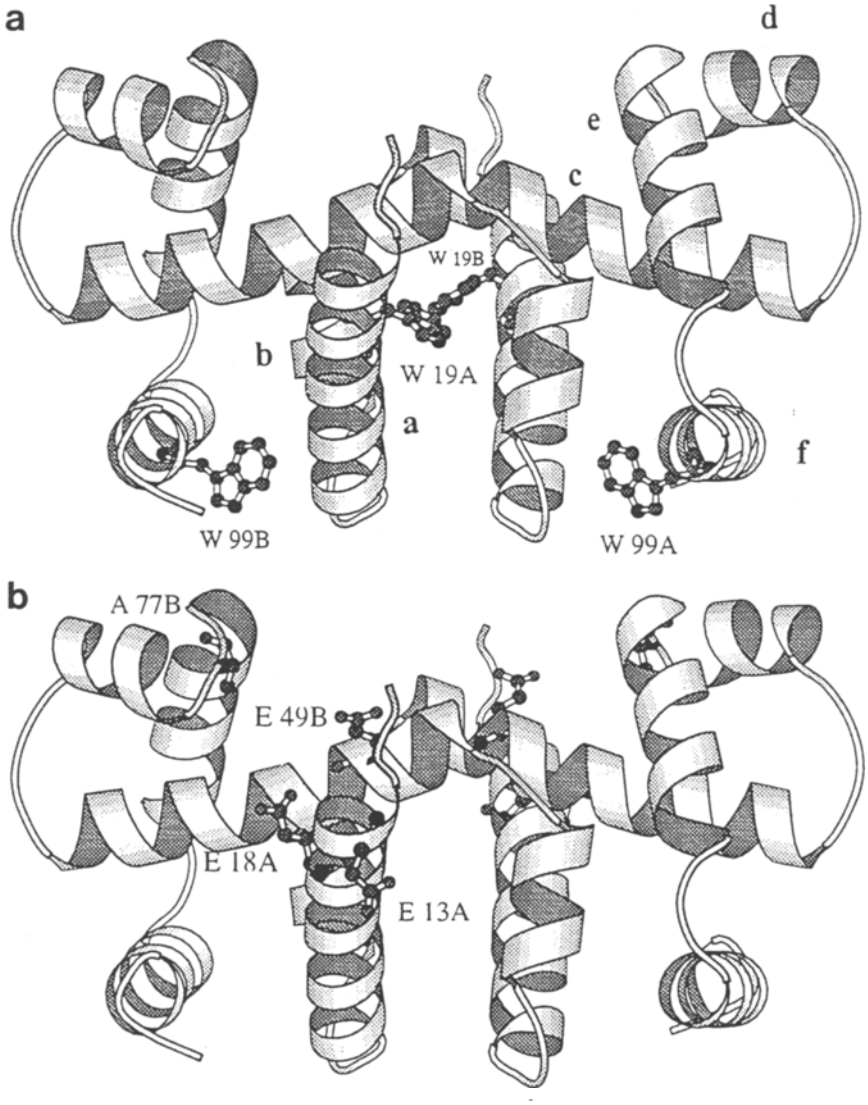

Fig. 1. (a) Ribbon diagram of the apo form of *trp* repressor taken from the coordinates obtained from the coordinates obtained by crystallographic analysis [24]. The two intrinsic tryptophan residues of each subunit are shown in ball-and-stick representation and labeled W19 and W99 A and B for chains A and B, respectively. The helices are labeled for one subunit a–f in lowercase to avoid confusion with the uppercase A and B denoting the two monomer chains. (b) Ribbon diagram of *trp* repressor [24] showing the positions of the superrepressor mutations, EK13, EK18, EK49, and AV77. Figures were generated using the program Molscript [55].

[21,23] have shown that the AV77 mutation leads to an ordering of the D and E helices due to the additional hydrophobic bulk of the added methyl group at this C-cap position of helix D. The substitutions at position 13, 18, and 49, likewise lead to differences in the secondary structure of the protein [22], but these are less readily interpretable than that for the AV77 mutant, since the CD spectra indicate the presence of a β-turn structure in these mutants. Moreover, the higher-order oligomerization of *trp* repressor dimers is perturbed for these mutations. Unfolding experiments on these mutants demonstrated that the AV77 mutant is more stable than the WT, with the same apparent cooperativity of unfolding, whereas the charge change mutants unfold at a lower denaturant concentration, but with a higher apparent cooperativity, such that the unfolding free energies are similar to that obtained for the wild type [21,22]. Isothermal titration calorimetry on tryptophan (corepres-

sor) binding to these mutants revealed that although the affinities are similar to the binding by the wild type, the underlying energetics are very different. The combination of these observations indicates that subtle, yet significant structural and dynamic modifications result from these single-site amino acid substitutions, which in turn lead to significantly altered activity *in vivo*. Below we present the characterization of the intrinsic fluorescence decay of these superrepressor mutants in the native and denatured states of these proteins and discuss the structural basis for the observed differences in the decays.

MATERIALS AND METHODS

Steady-State Fluorescence Techniques

Steady-state emission spectra of the intrinsic tryptophan fluorescence were collected in a quartz cuvette on an ISS KOALA spectrofluorometer (ISS, Champaign, IL) with an excitation wavelength of 295 nm and the emission wavelength scanned from 315 to 450 nm with an 8-nm bandpass in both excitation and emission. The background spectra were also collected using solutions identical to the samples except for the absence of protein. The sample spectra were corrected by subtracting the background spectra from the sample spectra.

Fluorescence Lifetime Determination

Phase angle and modulation measurements were carried out as a function of frequency relative to *p*-terphenyl in cyclohexane, which has a lifetime of 1 ns [28] using ISS frequency domain acquisition electronics. The excitation light polarized at 35° was at 295 nm from the frequency-doubled output of a Coherent cavity dumped 701 dye laser excited with the 532 line of a Coherent frequency-doubled mode-locked ND–YAG Antares laser (Coherent Corp., Palo Alto, CA). The errors for phase and modulation data were less than 0.3° and 0.005 modulation unit, respectively. The data for each sample were collected at 320, 340, 360, 380, and 400 nm using the ISS KOALA monochromator with slits set at a bandpass of 8 nm. The experiments were done with proteins in their native and denaturated states. For the samples of native proteins, the solutions were prepared in the absence of guanidine hydrochloride, while for the denatured state guanidine hydrochloride at a concentration of 4 *M* was added. For AV77, due to its higher stability, the solutions contained 6 *M* guanidine hydrochloride. Mutant proteins were produced from the plasmids and strains obtained from Dr. Charles Yanofsky and purified as described previously [21,22]. The protein concentrations were between 1 and 3 μM and were determined by absorption measurements at 280 nm. The extinction coefficients of the mutants were determined in 6 *M* urea as described in our earlier work [21,22].

The frequency–response curves were analyzed with the global analysis software developed by Beechem and co-workers [29]. The phase and modulation data were fit assuming multiexponential decay as described below:

$$I(t) = \sum_i \alpha_i e^{-t/\tau i} \quad (1)$$

where α_i is the preexponential factor, τ_i is the fluorescence lifetime, and $I(t)$ is the intensity at time, t. For analysis of the emission of each of the TR variants as a function of emission wavelength, the frequency–response curves for a particular mutant were analyzed simultaneously using a model in which the three lifetimes were floating parameters in the fit but were linked (invariant) across emission wavelength. Fractional intensities for each component, used to calculate the intensity of each component at each wavelength, were obtained from the preexponential factors using the relation.

$$f_i = \alpha_i\tau_i / \sum_i \alpha_i\tau_i \quad (2)$$

Differential Polarization

The time-dependent decays of fluorescence anisotropy were investigated using differential phase fluorometry. Essentially, the phase and modulation difference between the perpendicular and the parallel components of the emission is measured as a function of frequency, exciting the samples with vertically polarized, sinusoidally modulated light using a 340-nm-bandpass filter for emission [30]. Lifetime measurements were also made for all the samples using a 340-nm bandpass filter. The differential polarization data were analyzed using a simple nonassociative model of three lifetimes and two rotational correlation times, with the lifetime values obtained under the same conditions as fixed parameters in the fits. The time-resolved anisotropy $r(t)$ can be expressed as

$$r(t) = (i_\parallel(t) - i_\perp(t))/(i_\parallel(t) + 2i_\perp(t)) \quad (3)$$

where

$$i_\parallel(t) = 1/3 \sum_i \alpha_i \exp(-t/\tau_i) [1 + 2\sum_j \beta_j L_{ij} \exp(-t/\phi_j)] \quad [4]$$

and

$$i_\perp(t = 1/3 \sum_i \alpha_i \exp(-t/\tau_i) [1 - \sum_j \beta_j L_{ij} \exp(-t/\tau_j)] \quad (5)$$

and where

i = 1, number of lifetime components
j = 1, number of rotational rates

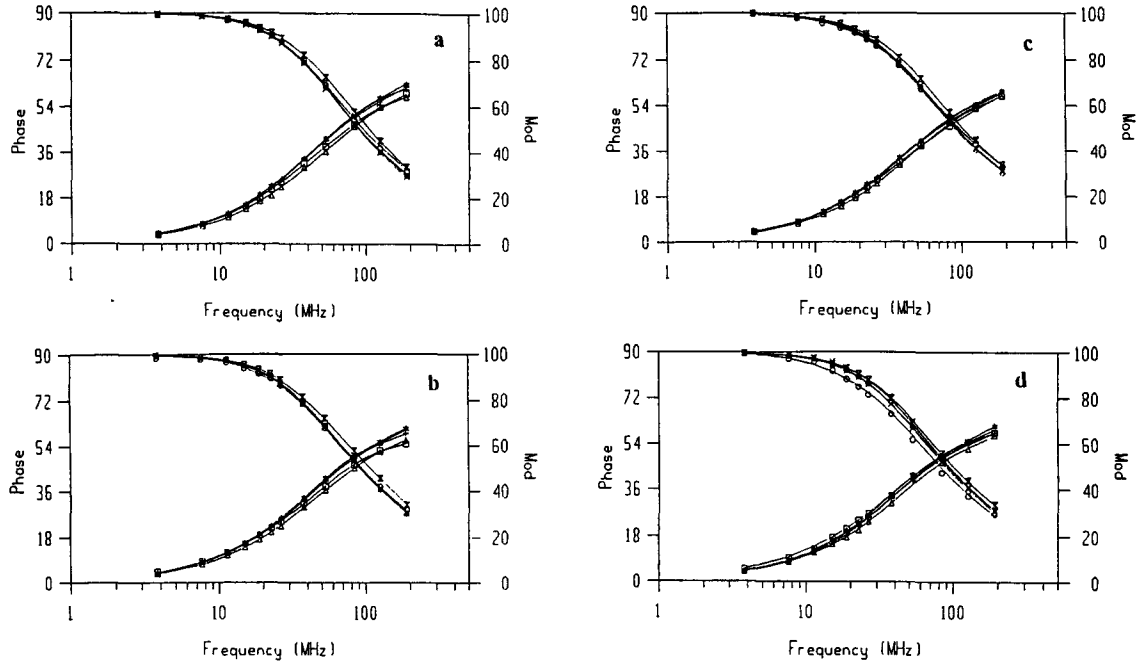

Fig. 2. Comparison of the frequency–response profiles of the native states of WT TR and the superrepressor mutants at (a) 320 nm, (b) 340 nm, (c) 360 nm, and (d) 380 nm. Symbols are given for the phase and modulation data of each TR variant, respectively, as follows: + and x, WT; □ and ○, EK13; △ and ⧖, EK18; ⋆ and ◇, EK49; + and x, AV77. Excitation was at 295 nm and emission was monitored through an ISA monochromator with a 16-nm bandpass. The proteins were dissolved in 10 m*M* phosphate buffer, 100 m*M* KCl, 0.1 m*M* EDTA, pH 7.6. The temperature was regulated at 21°C.

In an associative model, $L_{ij} = 1$ for all crossterms of τ_i and ϕ_j. The limiting anisotropy was also a floating parameter in the fit and was recovered to be approximately 0.23. The concentration of protein for these measurements was between 4 and 10 μ*M*.

Buffer Conditions

All the measurements for TR were made in 10 m*M* phosphate buffer at pH 7.6, 0.1 m*M* EDTA, and 100 m*M* KCl at 21°C, thermostated. High salt concentrations were used since it is known from previous studies [22,31] that at higher salt concentrations, the oligomerization of apo TR is disfavored, and at 100 m*M* KCl, the proteins are predominantly in the dimeric form. Moreover, time-resolved fluorescence dilution profiles have revealed identical frequency response profiles for the oligomerized as for the dimeric form of WT TR (C. A. Royer, unpublished results).

RESULTS

The steady-state fluorescence emission spectra of the superrepressor mutants of TR were indistinguishable from that obtained for the wild type (data not shown), indicating that no large differences in solvent exposure of either tryptophan results from the mutation. The frequency–response profiles for native WT TR and the superrepressor mutants were obtained at multiple wavelengths in order to decompose the various decay components by their color as well as their lifetime. In the presentation of these results, we feel that it is important to stress the differences and similarities in the raw data between the mutants and the wild type before discussion of the values of the parameters recovered from the various fits of the data. Figures 2a–d show the frequency–response curves for WT TR and each of the superrepressor mutants, EK13, EK18, EK49, and AV77, obtained at each of four emission wavelengths, 320, 340, 360, and 380 nm. It can be seen from these data that only the substitutions at positions 13 and 18 (squares, EK13, and triangles, EK18—phase; circles, EK13, and hourglass, EK18—modulation) give rise to significant differences in the frequency–response profiles, and these are most pronounced on the blue edge of the spectrum. Since these substitutions are in the A helix and, in the case of position 18, right next to tryptophan 19, it is likely that the shorter average lifetimes (as deduced from the shifts of the frequency–response curves to higher fre-

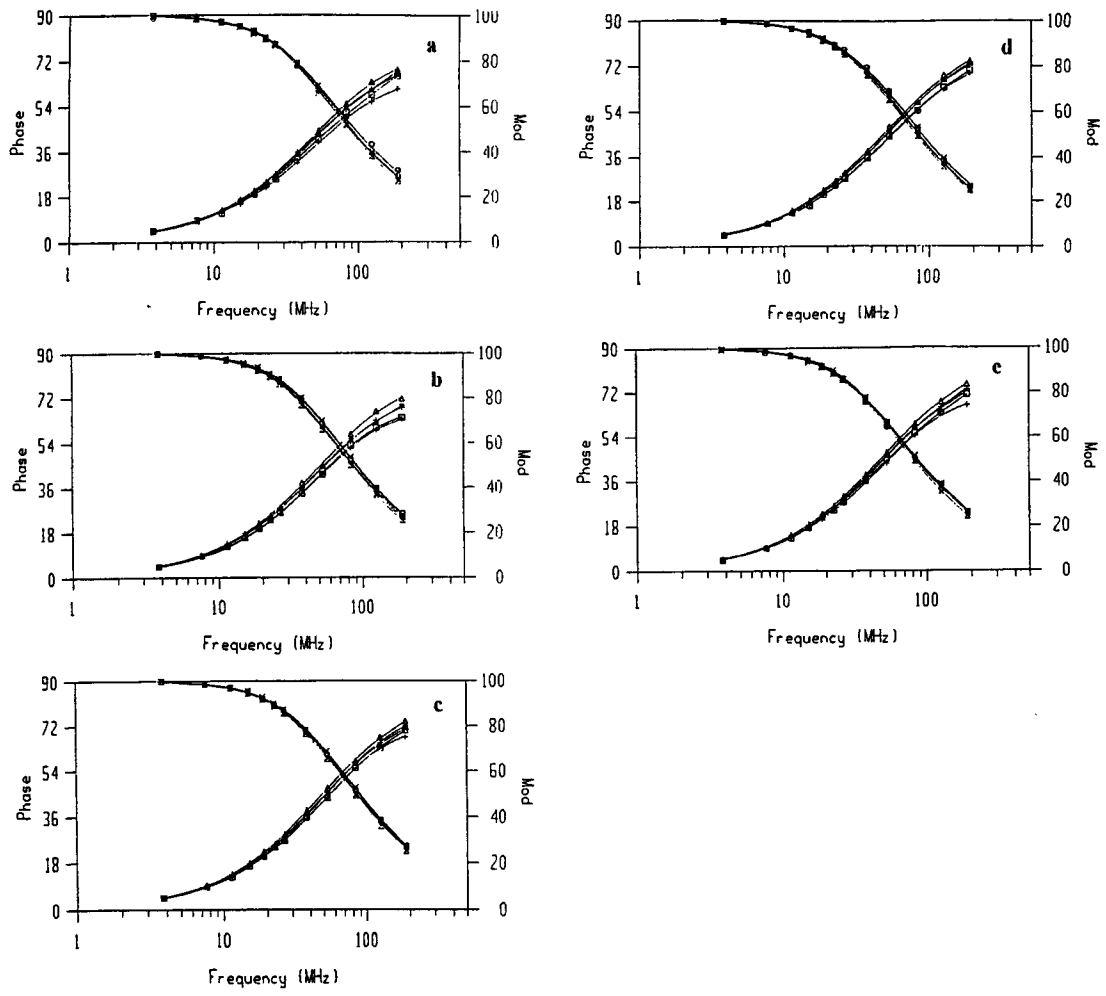

Fig. 3. Comparison of the frequency–response profiles of the denatured states of WT TR and the superrepressor mutants at (a) 320 nm, (b) 340 nm, (c) 360 nm, (d) 380 nm, and (e) 400 nm. Symbols are given for the phase and modulation data of each TR variant, respectively, as follows: + and x, WT; □ and ○, EK13; △ and ⧖, EK18; ⋆ and ◇, EK49; + and x, AV77. Excitation was at 295 nm and emission was monitored through an ISA monochromator with a 16-nm bandpass. The proteins were dissolved in 10 m*M* phosphate buffer, 100 m*M* KCl, 0.1 m*M* EDTA, pH 7.6, with 4 *M* GuHCl, except in the case of AV77, which requires 6 *M* GuHCl for denaturation. The temperature was regulated at 21°C.

quencies) arise from perturbations of the decay of tryptophan 19 (rather than tryptophan 99) by the mutations.

The frequency–response curves for the mutants in comparison with WT TR under denaturing conditions (as described under Materials and Methods) are shown in Figs. 3a–e for 320, 340, 360, 380, and 400 nm. The emission spectra of the mutants and WT TR under these conditions were identical. However, contrary to what one may have expected, the differences in the frequency–response profiles between WT TR and the mutants are more pronounced than they are in the native state. The wild-type response is clearly shifted to a higher frequency (crosses in phase; x's in modulation), particularly at 320 nm, as compared to the mutants. For example, the frequency–response profiles of the AV77 and EK49 mutants in the native state were nearly identical to that of WT TR, but in the denatured state their decays are on average longer-lived than WT TR. EK13, on the other hand, exhibited an upshifted frequency response (shorter decay) compared to WT TR in the native state but is nearly identical in the denatured state. Finally, the EK18 mutation, which resulted in a significantly shorter-lived emission in the native state, exhibits a significantly longer one in the denatured state. In all cases the denatured state decays were longer on average than those of the native state and were also more heterogeneous. It is noteworthy that in the denatured state, the frequency–response profiles of the mutants are dis-

Table I. Results of the Decay-Associated Spectra Analysis of WT and Superrepressor Mutants of TR in the Native State

Protein	τ (ns)	Fractional intensity 320 nm	Fractional intensity 380 nm
WT			
τ1	12	0.01	0.01
τ2	3.3	0.85	0.83
τ3	0.6	0.14	0.16
EK13			
τ1	7.1	0.09	0.26
τ2	2.9	0.77	0.60
τ3	0.5	0.14	0.13
EK18			
τ1	4.6	0.17	0.38
τ2	2.6	0.70	0.50
τ3	0.4	0.13	0.13
EK49			
τ1	11	0.00	0.10
τ2	3.4	0.86	0.74
τ3	0.7	0.14	0.16
AV77			
τ1	4.3	0.40	0.52
τ2	2.6	0.48	0.35
τ3	0.5	0.12	0.13

Table II. Results of the Decay-Associated Spectra Analysis of WT and Superrepressor Mutants of TR in the Denatured State

Protein	τ (ns)	Fractional intensity 320 nm	Fractional intensity 380 nm
WT			
τ1	7.2	0.08	0.13
τ2	3.0	0.81	0.82
τ3	0.4	0.11	0.05
EK13			
τ1	4.5	0.37	0.49
τ2	2.4	0.57	0.48
τ3	0.4	0.06	0.02
EK18			
τ1	4.7	0.30	0.42
τ2	2.7	0.68	0.58
τ3	0.2	0.02	0.00
EK49			
τ1	6.7	0.06	0.10
τ2	3.1	0.86	0.87
τ3	0.6	0.08	0.03
AV77			
τ1	4.1	0.53	0.58
τ2	2.5	0.39	0.41
τ3	0.6	0.07	0.01

tinct from that of the denatured WT TR. This suggests that the conformations of proteins in the denatured state may present a certain degree of specificity. The purification of all of these proteins yielded single bands on Coomasie-stained gels, but one can never exclude contributions from contaminating proteins. Nonetheless, since these differences in emission characteristics depend upon the conditions of the experiment, it is unlikely that they arise from contaminants. No blank subtraction was carried out for the time-resolved measurements, as this is not possible in our setup. However, all data were obtained under identical conditions (denaturant concentration, buffer concentration, protein concentration) except for AV77, which required a higher concentration of denaturant. Thus, the differences in the frequency response of AV77 could arise from contaminants in the GuHCl, but this could not explain the differences observed between denatured WT TR and EK18. Moreover, most of the background signal arises from leaked scattered light, which is constant from sample to sample, not from GuHCl contaminants, as the background steady-state spectra are nearly identical for pure buffer and buffer containing high concentrations of GuHCl.

We have previously resolved the contributions of the individual tryptophan residues, 19 and 99, to the overall fluorescence decay of native WT TR using single-tryptophan mutants [18,19], and these previous results are described in the Introduction. Tryptophan 19 is blue-shifted ($\lambda_{max} \approx 319$ nm), with a 4- and a 2.5-ns component, while tryptophan 99 is redder in its emission ($\lambda_{max} \approx 340$ nm) with a 0.5- and a 2.5-ns decay. In analyses of the decay of WT TR, which contains both tryptophan residues, the two components near 2.5 ns for the two tryptophan residues are indistinguishable. Typically, best fits of the WT decay are obtained with three-component models in which the 0.5-ns component is well resolved and in which two longer components are recovered. Depending upon the wavelength of observation, their values range from 4 to 12 ns for the long component and from 2.5 to 3.5 ns for the intermediate lifetime. In fact, the WT decay, as we published earlier [18], also fits well to a well-resolved short 0.5-ns component plus a distributed long component with a maximum near 3 ns and whose width varies with emission wavelength.

In Tables I and II are given the values of the lifetimes and fractional intensities resulting from a triple-exponential analysis of each of the proteins individually in either the native (Table I) or the denatured (Table II) state, in which the lifetimes were linked across emission wavelengths. For reasons of brevity only the fractional intensities at 320 and 400 nm are given, to allow comparison between the blue and the red edge of the spectrum. Surveying the values obtained from the analysis, the 5, 2, 0.5 rule appears to apply in all cases. However,

we know, at least for the wild type in the native state, that this represents in reality a superposition of the decays of two tryptophan residues that do not follow this rule individually. The most well-resolved feature of these decays is the shortest 0.5-ns component, due to tryptophan 99 in the native state. In fact, its fractional contribution to the total intensity of all of the native proteins is invariant with wavelength. However, the short component recovered from the unfolded state analysis is systematically blue shifted in its contribution, and we know from analysis of the unfolding of the W19F mutant that it is not present in the unfolded state when only tryptophan 99 is present in the structure [19]. Thus, we propose that this short component arises from tryptophan 99 in the native state, as previously reported, but from tryptophan 19 in the denatured state.

Analysis using the lifetime linked model of the native state decays of WT, EK13, and EK49 yielded a small fraction of a very long component (7–12 ns), a majority of the intensity from a 3-ns component, and then the well-resolved component at 0.5 ns. The results from EK18 and AV77 were closer to those obtained with prior knowledge that the decay actually is a superposition of two lifetime components from each tryptophan, yielding a component near 4.5 ns, another near 2.5 ns, and finally, the well-resolved 0.5-ns component. Upon examination of the recovered values, there appear to be two distinct trends in the results, but in terms of raw data, the frequency–response profiles of AV77 and EK49 were both nearly identical to WT at all wavelengths. We point this out as a cautionary note to indicate that very small differences in raw data can give rise to apparently large differences in recovered parameters, which reflect a very subtle bias in the data. It is for this reason that, prior to any analysis, we examine the raw data to determine if any significant difference in the decay between the wild type and mutants truly exists.

We have also investigated the rotational properties of the tryptophan residues of these mutants in the native state. Eftink and co-workers [20] have shown for WT TR that tryptophan 19 exhibits almost no rotational freedom on the fluorescence time scale, while tryptophan 99 exhibits a fast rotational component. Comparison of the differential polarization results for WT TR and the four superrepressor mutants analyzed in terms of two rotational rates, with a simple nonassociative model (as described under Materials and Methods) shows that the rotational properties of the intrinsic tryptophan residues of these proteins (WT TR and mutants) are experimentally indistinguishable (data not shown). All exhibit a long correlation time of about 16 ns, consistent with a dimer of the size and shape of TR [32]. In addition, consistent with the results of Eftink and co-workers [20], about 20% of the depolarization is due to a fast rotation of about 1 ns, assigned by these previous investigators to tryptophan 99. Although one could analyze the differential polarization data with a more complex associative model, the point here is that, as in the case of the emission energy, the mutations appear to cause no significant difference in the mobility of the individual tryptophan residues.

DISCUSSION

We have examined the fluorescence decay characteristics of four single-site mutants of the *trp* repressor that result in significant structural and functional modifications of the protein. For the AV77 mutant, profound structural changes representing an approximate 50% increase in helicity of the HTH DNA binding domains [21] results in almost no difference in the intrinsic tryptophan fluorescence in the native state. This is understandable, since neither tryptophan is near the helix–turn–helix domain of the protein. However, interestingly, a significantly longer fluorescence lifetime is observed for the AV77 mutant in the denatured state as compared to WTTR. Previous unfolding studies of AV77 indicated that the same amount of surface area was exposed upon unfolding of this mutant, compared to the wild type [21], since the apparent cooperativity or m value of the urea and guanidine unfolding profiles is identical [33]. Since the AV77 mutant is significantly more structured in the native state than WT TR and buries a significantly greater surface area, we concluded that there must be, as well, differences in the exposed surface area of this mutant in the denatured state, compared to WT TR. The fact that we observe differences in the fluorescence decay between AV77 and WT TR in their denatured states supports the notion of distinct denatured conformations. The EK49 mutant exhibited a similar trend in the fluorescence decays as the AV77 mutant. The secondary structure of this mutant is also different than WT TR in the native state, but like AV77, EK49 exhibits decay characteristics identical to WT.

The EK13 mutant, on the other hand, presents a shorter-lived decay than WT TR in the native state, but is nearly identical to WTTR in the denatured state. Previous CD measurements on native EK13 indicated that some β-turn structure is introduced by the mutation [22], and we have postulated that this substitution may order the N-terminal arms of the repressor, which are not resolved from the X-ray crystallographic data, except in the case of the structure of tandem dimers bound to a

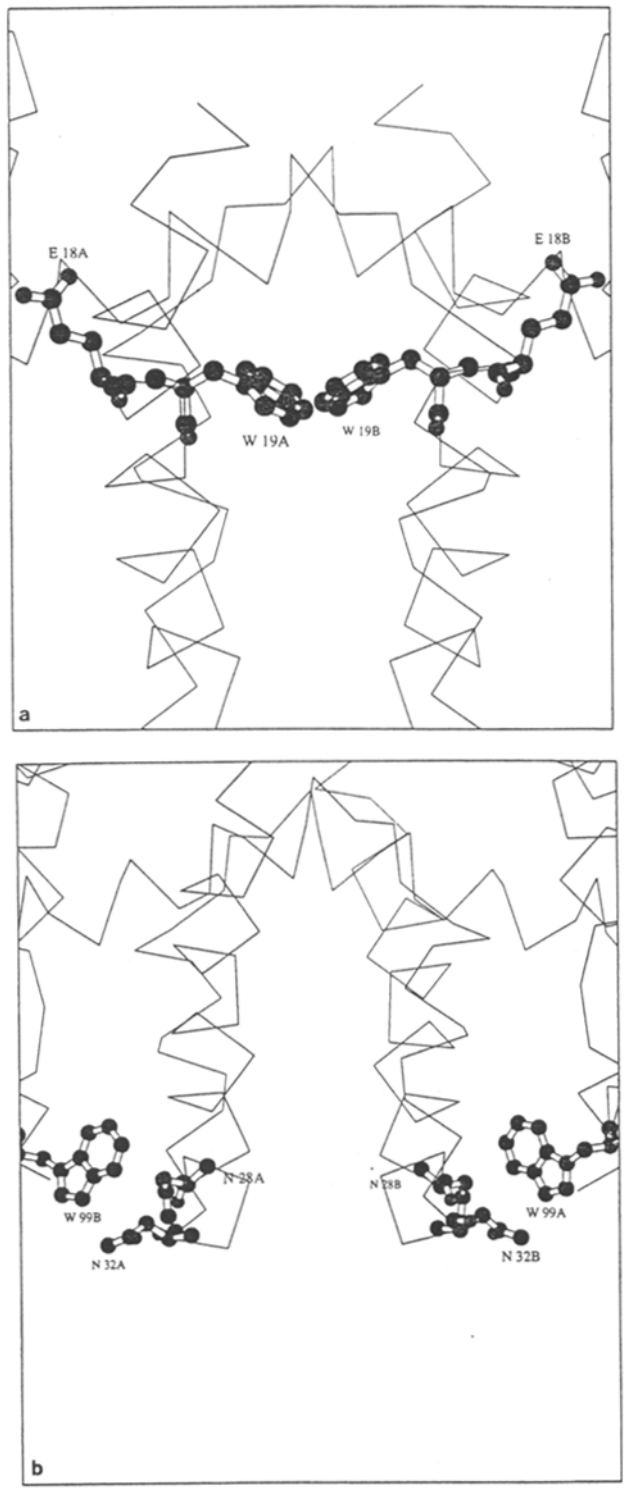

Fig. 4. Closeup view of the tryptophan residues of TR (ball-and-stick representations). (a) Tryptophan 19 and glutamate 18. Note that the side chain of E18 points in the opposite direction from W19. (b) Tryptophan 99. Also shown are asparagine 28 and 32. Taken from the coordinates of the three-dimensional crystal structure of the aporepressor [24]. Figures were generated using the program Molscript [55].

single central operator half-site [34]. In this structure the N-terminal arms fold back into the core of the protein. The fact that the fluorescence decay is shorter in the native state, particularly on the blue edge of the spectrum, for this mutant is consistent with a subtle structural modification affecting tryptophan 19, since tryptophan 19 is the bluest of the two tryptophan residues.

The most significant differences observed between the fluorescence decay characteristics of this series of mutants and WT TR was observed, not surprisingly, for the EK18 substitution, adjacent to tryptophan 19. Significant differences were observed in both the native and the denatured states. Like the EK13 mutant, in the native state EK18 exhibited a shorter decay than WT TR, particularly on the blue edge of the spectrum, implicating effects of the mutation on tryptophan 19. That substitution of a glutamate by a lysine in proximity to a tryptophan residue would result in a decrease in the fluorescence lifetime is not surprising. However, this region is highly α-helical, and as shown in Fig. 4a, the side chain of glutamate 18 in the native structure points in the opposite direction of that of tryptophan 19. Thus, even given a certain degree of mobility of both residues in the helix, it is unlikely that the observed quench results from direct collision between lysine 18 and tryptophan 19. This region of the protein is extremely stable, and it is highly unlikely that local fluctuations include any significant unraveling of the helix, which would be necessary for a direct collisional quench of tryptophan 19 by the neighboring lysine. In the unfolded state, the decay of EK18 was significantly longer than that of WT TR. This result was surprising, since in the unfolded state, one would assume that the greater mobility might allow for direct, efficient collisional quenching to occur. We suppose that in both the native and the unfolded states, the mutation results in alterations of the general electrostatic environment or in the position and dynamics of the residues in this region. The changes we have observed in the CD spectrum of EK18 compared to WT TR support this hypothesis [22].

The rotamer form of the side chain of tryptophan 19 in the native structure as determined by X-ray crystallographic studies [24] is in the tp^- rotamer orientation. In fact, the *t* rotamer for the χ^1 bond is favored in α-helices [35]. Willis *et al.* [10] have postulated that the *t* rotamer population gives rise to the often observed long (≈5-ns) fluorescence decay time for tryptophan in proteins, while the intermediate decay time may correspond to the *g* rotamer, and the highly unfavorable (in an α-helical context) g^- rotamer would give rise to the shorter decay time. Such an explanation may be plausible for tryptophan 19. In this case, the 0.5-ns component would

be absent because the g^- rotamer is never populated in this very stable helix. However, then one would have to postulate a significant population in solution of the g^+ rotamer (nearly 50%) according to the amplitude (not fractional intensity) of the intermediate decay. Since this tryptophan exhibits no significant motion on the nanosecond time scale [20], such a possibility appears unlikely, although not impossible.

Tryptophan 99, also in an α-helix, is found in the tp^+ rotameric form in the structure derived from the crystallographic data [24]. It should then, in principle, exhibit the long decay time. However, this is not the case, as it exhibits only two components, near 2.5 and 0.5 ns. In fact, the amplitude of the short decay time (the well-resolved 0.5-ns component) represents over 50% of the tryptophan 99 residues [18]. We have proposed that this short component is not due to the population of the g^- rotamer, which would be quenched by contact with the peptide bond [36], but rather arises from quenching by one or two nearby asparagine residues, in the complementary subunit (see Fig. 4b). Upon unfolding, this 0.5-ns component disappears. Such behavior would not be expected for the g^- rotamer, which should be more favorable in a random coil configuration than in a helical one. However, as we have suggested previously [19], the disruption of subunit interactions would abrogate the quenching of tryptophan 99 by asparagine residues in the opposite subunit and the 0.5-ns component would disappear, rather than appear, upon unfolding.

There are other notable exceptions to the 5, 2, 0.5 (t, g^+, g^-) rule of thumb. The solvent-exposed tryptophan 220 of *lac* repressor, for example, has a dominant lifetime component near 9 ns [37,38], and that of liver alcohol dehydrogenase is also quite long [39]. The radiative lifetime of NATA in water is 20 ns [40]. On the other hand, the buried tryptophan of holoazurin is highly quenched by the copper [41–44]. The intrinsic fluorescence of heme proteins is usually dominated by extremely short lifetimes, <100 ps, due to energy transfer to the heme prosthetic group [45,46]. Disulfides [47,48] and amines [49,50] are also efficient quenchers of tryptophan fluorescence, such that their proximity can dominate the decay of native proteins.

Nonetheless, one often observes the 5-ns component for tryptophan residues that exhibit little or no rotational mobility. Apoazurin tryptophan decay kinetics fit well to a single-exponential model with a recovered lifetime near 5 ns [42,43]. This tryptophan displays extremely blue-shifted emission due to a uniquely hydrophobic environment and little rotational freedom [41]. The single tryptophan residue, W140, of staphylococcal nuclease is found in the t rotamer form for the χ^1 bond and is sandwiched between the methylene groups of two lysyl sidechains, 133 and 110 [51]. Although it is the last residue resolved in the structure deduced from X-ray data [51], it has been shown by our group and others [52–54] to exhibit little, if any, rotational freedom on the fluorescence timescale. Interestingly it decays as a near-single-exponential decay in the native state with a lifetime near 5–6 ns, particularly in the context of stabilizing proline-to-glycine mutations [53]. In the unfolded state, these nuclease variants exhibit the traditional triple-exponential decay (Vidugiris and Royer, unpublished results). Nearly single-exponential decay characteristics with a lifetime of near 5 ns have also been observed for a single tryptophan mutant of phage T4 lysozyme (trp138) when an additional substitution is made of an alanine for a glutamine residue at position 105 that hydrogen bonds to and quenches tryptophan 138 in the WT protein [17].

Given the effects reported here of single-site mutations on the tryptophan decays in both the native and the denatured states of TR, and prior characterization of the individual decays of the tryptophan residues in this and other proteins by a number of groups cited here, we have come to the general conclusion that rotamer populations serve to set the baseline properties of the fluorescence decay of tryptophan residues in proteins. Unlike folded proteins, peptides and unfolded proteins generally follow the 5, 2, 0.5 rule of thumb. Subtle effects of the surrounding sidechains are nonetheless still present even in the denatured states of proteins, as evidenced by the results presented here. In folded proteins, superimposed upon this baseline behavior are the tertiary interactions of the tryptophan with neighboring side chains in the three-dimensional structure, which can significantly alter (or even obscure) these baseline fluorescence decay characteristics.

ACKNOWLEDGMENTS

This work was supported by Grant GM39969 from the National Institutes of Health to C.A.R. We thank Dr. Charles Yanofsky for the plasmids bearing the *trp* repressor gene with the various superrepressor mutations.

REFERENCES

1. A. G. Szabo and D. M. Rayner (1980) *J. Am. Chem. Soc.* **102**, 554–563.
2. J. W. Petrich, M. C. Chang, D. B. McDonald, and G. R. Fleming (1983) *J. Am. Chem. Soc.* **105**, 3824–3832.

3. M. C. Chang, J. W. Petrich, D. B. McDonald, and G. R. Fleming (1983) *J. Am. Chem. Soc.* **105**, 3819–3824.
4. D. R. James and W. R. Ware (1985) *Chem. Phys. Lett.* **120**, 450–454.
5. R. A. Engh, L. X.-Q. Chen, and G. Fleming (1986) *Chem. Phys. Lett.* **126**, 365–372.
6. H. T. Yu, W. J. Colucci, M. L. McLaughlin, and M. D. Barkley (1992) *J. Am. Chem. Soc.* **114**, 8449–8454.
7. K. Doring, L. Onermann, T. Surrey, and F. Jähnig (1995) *Eur. Biophys. J.* **23**, 423–432.
8. R. F. Chen, J. R. Knutson, H. Ziffer, and D. Porter (1991) *Biochemistry* **30**, 5184–5195.
9. J. B. A. Ross, H. R. Wyssbrod, R. A. Porter, G. P. Schwartz, C. A. Michaels, and W. R. Laws (1992) *Biochemistry* **31**, 1585–1594.
10. K. J. Willis, W. Neugebauer, M. Sikorska, and A. G. Szabo (1994) *Biophys. J.* **66**, 1623–1630.
11. E. Bismuto, I. Sirangelo, and G. Irace (1991) *Arch. Biochem. Biophys.* **291**, 38–42.
12. J. B. A. Ross, C. A. Schmidt, and L. Brand (1981) *Biochemistry* **20**, 4369–4377.
13. P. H. Axelson, Z. Bajzer, F. G. Prendergast, P. F. Cottam, and C. Ho (1991) *Biophys. J.* **60**, 650–659.
14. N. D. Silva, Jr., and F. G. Prendergast (1996) *Biophys. J.* **70**, 1122–1137.
15. J. R. Alcala, E. Gratton, and F. G. Prendergast (1987) *Biophys. J.* **51**, 925–936.
16. Z. Bajzer and F. G. Prendergast (1993) *Biophys. J.* **65**, 2313–2323.
17. M. Van Gilst, A. Roth, and B. S. Hudson (1994) *J. Fluoresc.* **4**, 203–207.
18. C. A. Royer (1992) *Biophys. J.* **63**, 741–750.
19. C. A. Royer, C. G. Mann, and C. R. Matthews (1993) *Protein Sci.* **2**, 1844–1852.
20. M. R. Eftink, G. D. Ramsay, L. Burns, A. H. Make, C. J. Mann, C. R. Matthews, and C. A. Ghiron (1993) *Biochemistry* **32**, 8189–8198.
21. R. J. Reedstrom and C. A. Royer (1995) *J. Mol. Biol.* **253**, 266–276.
22. R. J. Reedstrom, K. S. Martin, S. Vangala, S. Mahoney, E. W. Wilker, and C. A. Royer (1996) *J. Mol. Biol.* **264**, 32–45.
23. T. H. Smith, Z. Zheng, and O. Jardetsky (1995) *Biochemistry* **34**, 13183–13189.
24. R.-G. Zhang, A. Joachimiak, C. L. Lawson, R. W. Shevitz, Z. Otwinowski, and P. B. Sigler (1987) *Nature* **327**, 591–597.
25. M. L. Tasayco and J. Carey (1992) *Science* **255**, 594–597.
26. L. Jin, J. Yang, and J. Carey (1993) *Biochemistry* **32**, 7302–7309.
27. R. L. Kelly and C. Yanofsky (1985) *Proc. Natl. Acad. Sci. USA* **82**, 483–487.
28. E. Gratton, M. Limkeman, J. Lakowicz, B. P. Maliwal, H. Cherek, and G. Laczko (1984) *Biophys. J.* **46**, 479–486.
29. J. M. Beechem, E. Gratton, M. Ameloot, J. R. Knutson, and L. Brand (1991) in J. R. Lakowicz (Ed.), *Fluorescence Spectroscopy: Principles and Techniques, Vol. 2*, Plenum Press, New York, pp. 241–306.
30. G. Weber (1977) *J. Chem. Phys* **66**, 4081–4091.
31. K. S. Martin, C. A. Royer, K. P. Howard, J. Carey, Y.-C. Liu, K. S. Matthews, E. Heyduk, and J. C. Lee (1994) *Biophys. J.* **66**, 1167–1173.
32. T. Fernando and C. A. Royer (1992) *Biochemistry* **31**, 3429–3441.
33. D. Shortle and A. K. Meeker (1986) *Proteins Struct. Funct. Genet.* **1**, 81–89.
34. C. L. Lawson and J. Carey (1993) *Nature* **368**, 178–182.
35. H. Schrauber, F. Eisenhaber, and P. Argos (1993) *J. Mol. Biol.* **230**, 592–612.
36. Y. Chen, B. Liu, H. T. Yu, and M. D. Barkley (1996) *J. Am. Chem. Soc.* **118**, 9271–9278.
37. J.-C. Brochon, P. Wahl, M. Charlier, J. C. Maurizot, and C. Hélène (1977) *Biochem. Biophys. Res. Commun.* **79**, 1261–1271.
38. C. A. Royer, J. Gardner, J. M. Beechem, J. C. Brochon, and K. S. Matthews (1990) *Biophys. J.* **58**, 363–377.
39. J. M. Beechem and L. Brand (1985) *Annu Rev. Biochem.* **53**, 43–71.
40. Y. Chen, B. Liu, and M. D. Barkley (1995) *J. Am. Chem. Soc.* **117**, 5608–5609.
41. A. G. Szabo, T. M. Stepanik, D. M. Wayner, and N. M. Young (1983) *Biophys. J.* **41**, 233–244.
42. C. M. Hutnik and A. G. Szabo (1989) *Biochemistry* **28**, 3923–3934.
43. J. W. Petrich, J. W. Longworth, and G. R. Fleming (1987) *Biochemistry* **26**, 2711–2722.
44. J. E. Hansen, J. W. Longworth, and G. R. Fleming (1990) *Biochemistry* **29**, 7329–7338.
45. Z. Gryyczynski, T. Tenenholz, and E. Bucci (1992) *Biophys. J.* **63**, 648–653.
46. K. J. Willis, A. G. Szabo, M. Zucker, J. M. Ridgeway, and B. Alpert (1990) *Biochemistry* **29**, 5270–5275.
47. A. Holmgren (1971) *J. Biol. Chem.* **247**, 1992–1998.
48. F. Mérola, R. Riegler, A. Holmgren, and J. C. Brochon (1989) *Biochemistry* **28**, 3383–3398.
49. M. Shinitzky and R. Goldman (1967) *Eur. J. Biochem.* **3**, 139–144.
50. R. Loewenthal, J. Sancho, and A. Fersht (1992) *J. Mol. Biol.* **224**, 759–7706.
51. T. R. Hynes and R. O. Fox (1991) *Proteins* **10**, 92–105.
52. P. Wu and L. Brand (1994) *Biochemistry* **33**, 10457–10462.
53. C. A. Royer, A. Hinck, S. Loh, K. Prehoda, P. Xiangdong, J. Jonas, and J. Markley (1993) *Biochemistry* **32**, 5222–5232.
54. M. R. Eftnik, I. Gryczynski, W. Wiczk, G. Laczko, and J. R. Lakowicz (1991) *Biochemistry* **30**, 8945–8953.
55. P. Kraulis (1991) *J. Appl. Crystallogr.* **24**, 946–950.